Hindawi
Advances in Civil Engineering
Volume 2019, Article ID 5152031, 17 pages
https://doi.org/10.1155/2019/5152031

Research Article

An Automated Procedure for Assessing Local Reliability Index and Life-Cycle Cost of Alternative Girder Bridge Design Solutions

Ilaria Venanzi,[1] **Riccardo Castellani**,[2] **Laura Ierimonti**,[1] **and Filippo Ubertini**[1]

[1]*Department of Civil and Environmental Engineering, University of Perugia, Via G. Duranti, 93-06125 Perugia, Italy*
[2]*Professional Engineer, Via V. Martinozzi, Giove, 86-05024 Terni, Italy*

Correspondence should be addressed to Ilaria Venanzi; ilaria.venanzi@unipg.it

Received 17 July 2018; Revised 21 November 2018; Accepted 9 December 2018; Published 20 January 2019

Academic Editor: Mariano Angelo Zanini

Stakeholders of civil infrastructures have to usually choose among several design alternatives in order to select a final design representing the best trade-off between safety and economy, in a life-cycle perspective. In this framework, the paper proposes an automated procedure for the estimation of life-cycle repair costs of different bridge design solutions. The procedure provides the levels of safety locally guaranteed by the selected design solution and the related total life-cycle cost. The method is based on the finite element modeling of the bridge and uses design traffic models as suggested by international technical standards. Both the global behavior and the transversal cross section of the bridge are analyzed in order to provide local reliability indexes. Several parameters involved in the design, such as geometry and loads and materials' characteristics, are considered as uncertain. Degradation models are adopted for steel carpentry and rebars. The application of the procedure to a road bridge case study shows its potential in providing local safety levels for different limit states over the entire lifetime of the bridge and the life-cycle cost of the infrastructure, highlighting the importance of the local character of the life-cycle cost analysis.

1. Introduction

Road infrastructures represent an important public asset and require large public expenditure for their construction and maintenance. Several failures of bridges all over the world demonstrate that many pieces of the road networks in western countries need strengthening or renovation [1]. When designing new road bridges or retrofitting old ones, usually several design alternatives are available for a single structure that are often very different in terms of economic investment and safety level.

In the traditional design method, the first most economic design alternative, providing the prescribed safety level, is selected. In the last decade, a new design approach has become popular, designated as the life-cycle cost analysis (LCCA) method, that evaluates the expected cost for the whole life cycle of the bridge, accounting for initial costs, maintenance costs and direct and indirect costs related to repair and disposal in a probabilistic framework [2–10]. All the uncertainties involved in the problem can potentially be taken into account, like the uncertainty on load characterization, on structural parameters, on materials' resistance, and on damage occurrence [11–14]. Multiple hazards can be easily taken into account by the LCCA approach [15, 16].

The evaluation of repair costs requires the computation of failure probability that, for large structures such as road bridges, can be a very cost-expensive operation. Indeed, the failure probability has to be computed for several structural elements and for numerous limit states, accounting for a large number of uncertainties and load conditions. Life-cycle cost has been used to optimize structural solutions and bridge design [17–26], to optimize retrofitting solutions [27], or in order to optimize bridge management and the maintenance program [28–32]. Deterioration of the materials is also typically included, by considering time-variant strength degradation models [1, 33–39].

In the present paper, an automated procedure is proposed for the LCCA of road girder bridges. The life-cycle cost is related to failure probability which is locally and automatically computed over the entire bridge deck for several limit states. The procedure accounts for the main peculiarities involved in the girder bridge design. Material's degradation and several sources of uncertainty in load and strength quantification are considered. Design traffic actions on the bridge suggested by up-to-date standards are also adopted considering the interaction between deck and girder loads. Different construction phases of composite steel-reinforced concrete beams are analyzed. The procedure leads to the evaluation of the time-dependent reliability index and failure probability for all the considered limit states and in correspondence of each location along the deck and the girder. It also provides the expected life-cycle cost, thus allowing a quantitative comparison between different design alternatives. The main progress of the methodology with respect to the existing literature is the local character of the reliability assessment and the life-cycle cost analysis that allows to decide the priority of intervention that is strongly dependent on the structural details of the deck and on the material's degradation model. The rest of the paper is organized as follows: Section 2 presents the proposed procedure for automatic LCCA of bridges. Section 3 presents an illustrative case study, while the results of the numerical simulations are presented in Sections 4 and 5. Finally, some concluding remarks are given in Section 7.

2. The Proposed Procedure

The proposed procedure is a general automated tool for the LCCA of girder bridges which accounts for the main peculiarities involved in the girder bridge design. It can take into consideration the real actions on a structure, also accounting for interaction between deck and girder loads, different construction phases of composite steel-reinforced concrete beams, uncertainties in load and strength quantification, and materials' degradation models. The procedure leads to the evaluation of the reliability index and failure probability for all the considered limit states and in correspondence of each location along the deck and the girder. It also allows for the computation of the expected life-cycle cost, thus allowing quantitative comparison between different design alternatives.

2.1. Life-Cycle Cost Analysis for Girder Bridges. The expected life-cycle cost for a bridge can be expressed as

$$\mathrm{E}\left[C\left(t_{\mathrm{l}}\right)\right] = C_{\mathrm{I}} + \sum_{t=1}^{t_{\mathrm{l}}}\left[\frac{\mathrm{E}\left[C_{\mathrm{M}}(t)\right] + \mathrm{E}\left[C_{\mathrm{R}}(t)\right]}{(1+r)^{t}}\right], \quad (1)$$

where E[] is the expected value, C_{I} is the initial cost, C_{M} is the maintenance cost at time t after construction, C_{R} is the repair cost at time t after construction, t_{l} is the lifetime of the structure, and r is the discount rate.

The initial cost C_{I} includes charges for design, testing, expropriation, materials and construction, and it is usually assumed to be deterministic.

The maintenance cost C_{M} includes the cost for inspection and ordinary maintenance, performed at regular time intervals [5, 40]. It is often assumed, during the design phase, to be directly proportional to the construction cost, and it can be minimized by planning an optimal series of maintenance and inspection activities. Maintenance actions have a non-negligible influence on structural reliability. When a maintenance action is performed, the materials and the structural elements are reported to be in their original conditions with a consequent increase in reliability. Nonetheless, as the maintenance cost is weakly dependent on the specific structural solution, it can be neglected in the preliminary design phase when the aim is to compare different structural alternatives [2, 30, 41].

Rehabilitation or repair has to be carried out when the structure reaches a critical limit state [5, 42]. The direct repair cost is the amount spent for the structural retrofit and can be computed as a function of the failure probability. To compute the expected life-cycle repair costs, it is assumed that the structure is restored to its original condition after each occurrence of damage. Under this hypothesis, the LC repair cost of a structural element can be written as

$$\mathrm{E}\left[C_{\mathrm{R}}(t)\right] = \sum_{j=1}^{J}\sum_{k=1}^{K} P_{j,k}^{f}(t) n_j c_{\mathrm{R},j}, \quad (2)$$

where J is the total number of independent limit states j, K is the total number of relevant sections k along the structural members, $P_{j,k}^{f}$ is the time-dependent probability of failure for the j-th limit state at section k, $c_{R,j}$ is the repair cost for limit state j referred to a length L_j across the section depending on the limit state j, and n_j is the number of elements subjected to limit state j. Additionally, the social impact of a failure can be taken into account through indirect costs, representing all the losses hanging on the community for the closing or load-bearing capacity reduction of the bridge [19, 43]. Indirect costs refer to non-tangible charges for the community and can be splitted in time loss for road users, injuries or fatalities, and socio-economic losses due to local production decrease [17, 44]. As indirect costs are slightly dependent on the structural solution, they are neglected in the current study but could be easily included, if needed, in the proposed framework.

2.2. Outline of the Procedure. The outline of the procedure is shown in Figure 1.

In the proposed procedure, as it is common in a girder bridge design at the stage of preliminary structural analysis for comparing different design alternatives, a transversal analysis of the deck is performed at first (local analysis), followed by a longitudinal analysis of the girders (global analysis). With this aim, a simplified modeling of the structure is carried out in which the structure of the bridge is ideally divided into two interconnected parts: the deck and the girder, representing its local and global behavior,

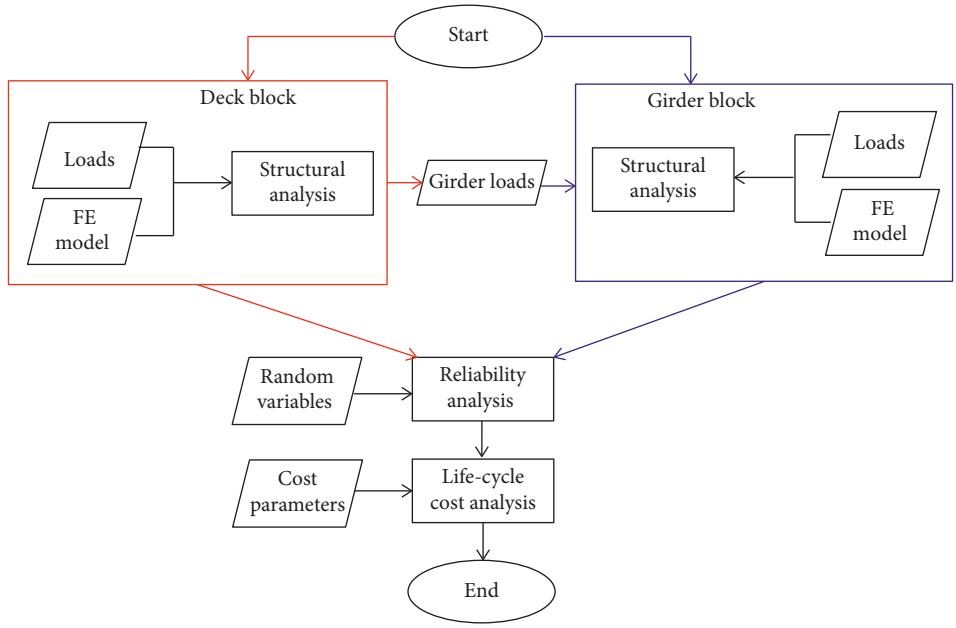

Figure 1: Outline of the proposed automated procedure.

respectively. The deck part is a modelization of the transverse section of the bridge, while the girder part is a modelization of the longitudinal, composite, reinforced concrete-steel girder. In the preliminary design phase, when the goal is to evaluate which is the best design alternative, the use of a simplified model instead of a complex finite element model is computationally advantageous and does not lead to relevant errors in the life-cycle cost evaluation.

In the deck analysis block, the FE model of the deck is assigned as input for the structural analysis which is repeated for each possible traffic load condition and position, to provide automatically the envelope of the internal forces.

In the girder analysis block, the FE model of the longitudinal beam is built and analyzed. It is loaded with constraint reactions of the deck structure corresponding to forces acting on girders provided by the deck analysis block, in addition to the other loads acting on the bridge, such as thermal actions and transverse loads. Then, a set of uncertain parameters, such as geometric data, materials' characteristics, and load intensities, are modeled as random variables with assigned probability distributions. Material's degradation can be considered by varying with time the geometric data and the properties of materials' strength. The reliability analysis is performed providing, locally in each section, the probability of failure and the corresponding reliability index for each output section of the deck and the girder. Finally, the life-cycle cost analysis is carried out by relating the probability of failure to the expected life-cycle cost of the analyzed bridge.

The procedure, built in a Matlab environment [45], requires the implementation of two FE models: one for the deck (in the deck analysis block) and one for the girder (in the girder analysis block). For each model, the discretization is chosen in order to differentiate between the different cross sections and between the sections with different reinforcements. Moreover, a sufficiently dense mesh has to be adopted in order to allow the movement of the concentrated or distributed loads over the structural elements. The envelope of stresses and displacements for moving loads is then computed in each section.

Courbon's method of analysis is adopted to properly allocate traffic loads between the girders. The girders are loaded with the maximum reactions obtained from the deck analysis.

The structural response is computed through static analyses for the three typical life phases of the steel-concrete mixed structure: construction, short term, and long term. Several types of loads are considered in addition to dead and traffic loads, like thermal action, transverse wind load, and centrifugal force. Results are directly provided for a preselected number of output stations along the deck and the girder.

Without loss of generality, to compute the failure probability $P_{j,k}^{f}(t)$ in equation (2), for each considered limit state and for each output station, the first order second moment method, i.e., the Hasofer-Lind procedure, is adopted. Probabilities of failure are calculated considering stochastic independence between all the involved random variables and treating them as normally distributed. In this way, the probability of failure is related to the well-known reliability index β, which represents the shortest distance of the selected limit state function from the origin of the reference system in the space of normal standard random variables. If random variables are not normally distributed but their distribution is approximately known, the first order second moment method can still be used by using equivalent normal random variables. As in the problem under investigation, the occurrence of limit states is checked locally, the reliability index depends on the output station k. It also

depends on the considered limit state j and on the time after construction ($\beta_{j,k}(t)$). Therefore, the failure probability can be computed as

$$P_{j,k}^{f}(t) = \Phi\left(-\beta_{j,k}(t)\right), \quad (3)$$

where Φ is the normal cumulative distribution function.

3. The Case Study Road Bridge

3.1. The Road Bridge and the Two Design Alternatives. The general procedure described in Section 2 has been applied for the design of a road bridge selected as the case study. It is a 550 m-long continuous steel-concrete composite viaduct with 10 spans with variable length. The deck width is 12.55 m including 9.75 m roadway and a 1.8 m sidewalk.

Two design alternatives of the viaduct are available: the first one corresponds to the original design, while the second one is a variant proposed by the contractor, leading to a reduction of the initial investment of about one million euros.

In alternative 1, the deck is a 30 cm thick concrete slab, supported by two steel box girders. The beams are stiffened and connected to each other at the supports with a steel plate. In alternative 2, the deck is a 26 cm thick concrete slab, supported by two double-T steel girders connected by transverse beams. The slab is designed as an equivalent beam with a plate behavior, thus guaranteeing that a thickness of 26 cm is sufficient to support the design loads. Figure 2 illustrates the transversal deck sections for both alternatives, in order to better understand the differences between the structural systems. The positions of the piers are different in the two design alternatives, as shown in Figure 3.

The strength class of concrete is C28/35 according to European guidelines [46] and the characteristic yield strength of reinforcement steel is 450 MPa. Steel S355 is used for the girders.

3.2. Finite Element Modeling. In order to carry out structural and reliability analyses, finite element models of the deck and the girders are built, for both design alternatives. Separate models have been adopted for the deck and for the main girder, as described in the following sections.

3.2.1. Deck Modeling. The deck has been modeled as a continuous reinforced concrete beam. For the deck analysis, the girders are considered as fixed supports, located in correspondence with the girders' axes. Figure 4 shows the deck modeling for the two design alternatives. The deck FE models for alternatives 1 and 2 are designated as D1 and D2, respectively. The nodes between the external supports are evenly spaced, at every 50 cm, in order to correctly reproduce traffic load positioning, with a limited computational effort. Noneven distribution of nodes is adopted for the sidewalks in order to account for the slab height variation and for the concentrated load positioning. Nodes are connected by beam elements with 3 degrees of freedom for each node. The displacements and the internal forces are computed not only in correspondence with the 24 joints of the model but also at intermediate sections between two adjacent nodes, for a total of 69 output sections.

Three different cross sections are assigned to the frames in D1, differing from each other in terms of slab thickness and reinforcements. Five different cross sections are assigned to the frames in D2, according the available preliminary design.

3.2.2. Girder Modeling. The girders are modeled as continuous beams, as shown in Figure 5. The girders are simply supported at piers and hinged at fixed abutments. These constraints reflect the behavior of the real supports to be used in the two design alternatives. The joints' locations are chosen to reproduce traffic load positioning, support location, and to account for reinforcement's variations. The girder FE models for alternatives 1 and 2 are designated as G1 and G2, respectively. Model G1 consists of 89 nodes, and model G2 consists of 107 nodes.

Stiffness properties have been calculated considering the different life phases of the steel-concrete composite structure:

(1) Phase1 (P1): the construction phase in which steel girders only contribute to resistance; loads due to girders and deck self-weight are applied

(2) Phase2 (P2): the short-term phase in which the concrete deck contributes to section resistance (modular ratio $n_0 = 6.18$, according to [47]); dead loads are applied

(3) Phase3 (P3): the long-term phase in which the concrete deck contributes to section resistance (modular ratio $n_L = 17.05$ [47]); dead and live loads are applied

Therefore, for each model (G1 and G2), three different model variants are considered, corresponding to the first, the second, and the third phases (G1-1, G1-2, G1-3, G2-1, G2-2, and G2-3). The effect of shrinkage is neglected, as shrinkage-reducing admixtures are used for the deck concrete.

3.3. Load Analysis. To properly describe the probabilistic nature of traffic loads, the load cases (self-weight, dead, and variable loads) have been treated separately.

Self-weights correspond to the weight of the reinforced concrete slabs and the steel girders. The dead loads include the weight of the pavement, the guard rail, and the parapet. The first one is a uniformly distributed load, while the other ones are concentrated loads. Variable loads are traffic loads and thermal fluctuation. The seismic action has not been considered at this stage of the work.

According to European guidelines [48, 49], different traffic load models are considered as follows:

Road traffic loads:

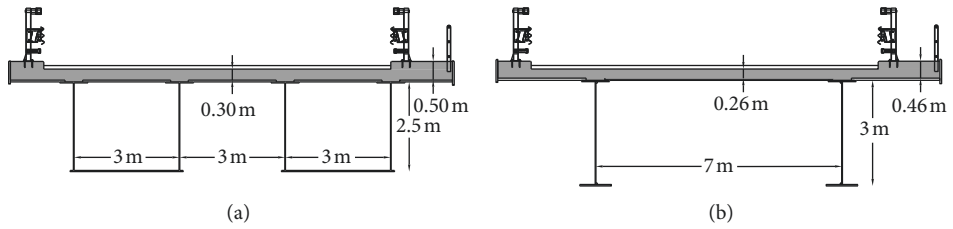

Figure 2: Cross sections of the two bridge design alternatives (D1 and D2).

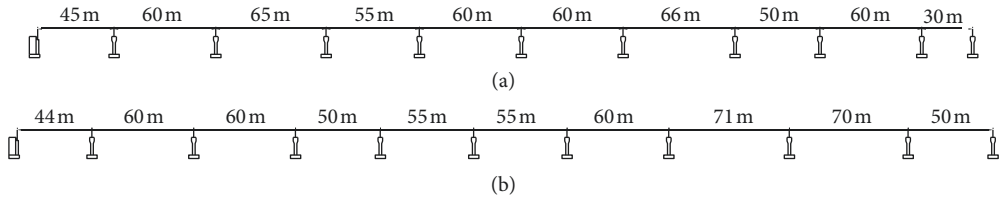

Figure 3: Longitudinal sections with span length of the two bridge design alternatives (G1 and G2).

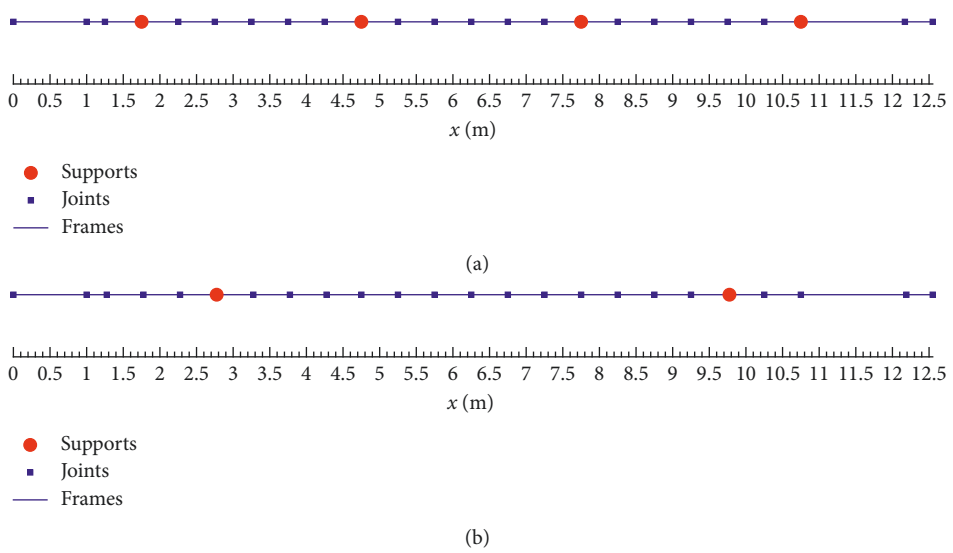

Figure 4: Schematic representation of the deck FE models in the two design alternatives. (a) Alternative 1: D1. (b) Alternative 2: D2.

(i) Load model 1 (LM1): concentrated and uniformly distributed loads, which cover most of the effects of the traffic of lorries and cars
(ii) Load model 2 (LM2): a single-axle load applied on specific tyre-contact areas which represents an exceptionally heavy vehicle and also the dynamic effects of the normal traffic on short structural members

Actions on footways:

(i) Uniformly distributed load (UDL): a uniformly distributed load, equal to 5 kN/m^2, for global verifications
(ii) Concentrated load (CL): a concentrated load on a square imprint having a 0.1 m side, equal to 10 kN, for local verifications.

In LM1, the roadway is divided into 3 equivalent lanes, 3 m wide. Any equivalent lane contains a distributed load acting over the whole lane width and two distributed loads, representing wheels of heavy vehicles, acting in a 0.4 m side square imprint to be diffused till half the deck thickness. LM2 consists of two 200 kN loads, on footprints of 0.6 m × 0.35 m, 2 m spaced, to be diffused till half the deck thickness. The worst load position along the roadway has to be considered. Values of lane loads, heavy vehicles wheel loads, number of equivalent lanes, and any other details on load models are given in [49].

For the deck analysis, the self-weight, the dead loads, and the load models LM1, LM2, UDL, and CL are considered. Figure 6 shows the applied loads for design alternative D1 (Figure 6(a)) and for design alternative D2 (Figure 6(b)). For the girder analysis, the following types of loads are

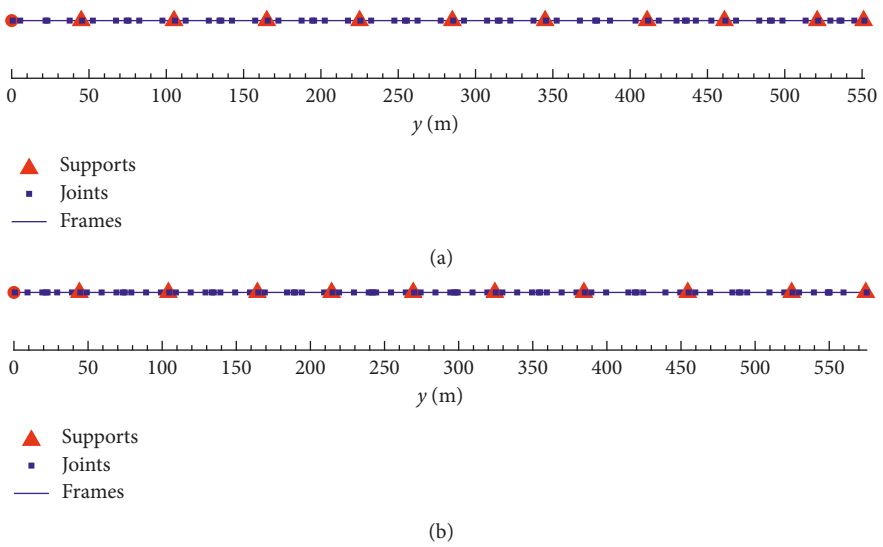

Figure 5: Schematic representation of the girder FE models in the two design alternatives. (a) Alternative 1: G1. (b) Alternative 2: G2.

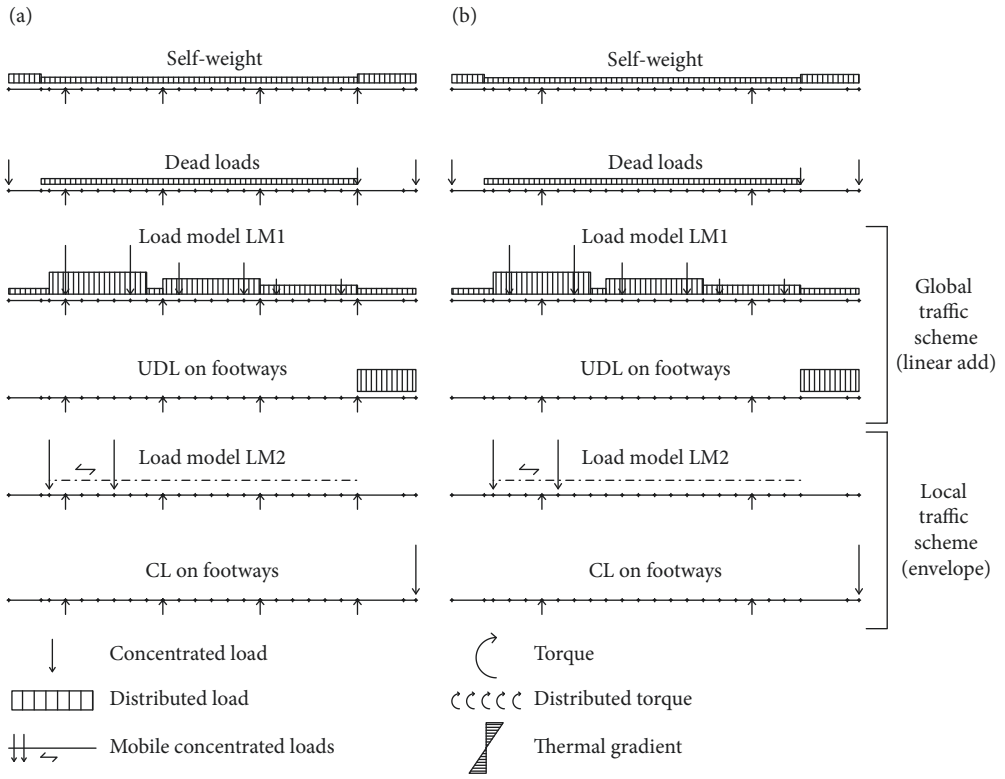

Figure 6: Schematic representation of the applied loads for the deck analysis. (a) Alternative 1: D1. (b) Alternative 2: D2.

considered acting on girders: the self-weight of deck and girder, the traffic loads (LM1), the thermal action, and the transverse loads due to wind. Deck self-weight and traffic loads are applied to the girders, by computing the constraint reactions acting on the deck. The analyses with LM1 in a limited number of spans have been omitted at this stage of the work since considering the favourable effect of LM1 would lead to a significant increase in the number of load cases and would not give an important contribution in the perspective of comparing different design alternatives.

Figure 7 shows the applied loads for design alternative G1 (Figure 7(a)) and for design alternative G2 (Figure 7(b)). The applied loads depend on the construction phase: in P1, only the girder and deck self-weight are considered, while in P2 and P3, dead loads, traffic loads, thermal action, and transverse loads are also taken into account. Traffic loads and deck self-weight produce different constraint reactions: in G1, the symmetrical component of the reactions produces a uniform bending of the box girder while the antisymmetrical one produces a torsion; in G2, the reactions produce a

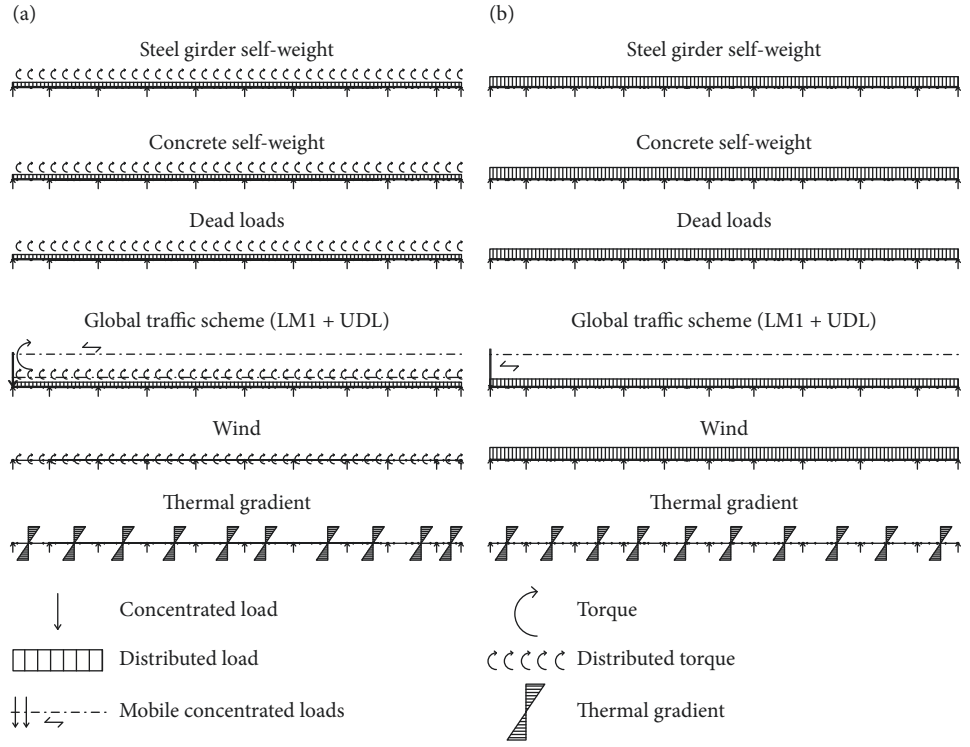

Figure 7: Schematic representation of the applied loads for the girder analysis. (a) Alternative 1: G1. (b) Alternative 2: G2.

uniform bending of the girders. Transverse loads consist in wind force and spin-dryer force applied by the vehicles running the 545 m radius curve. They produce a torsional moment due to the eccentricity between the point of application of the load and the geometric center of the deck that results in torque in the box girder in G1 and in a uniformly distributed vertical load on the girders in G2, given by the global torsion divided by the girders' distance.

3.4. Random Variables and Degradation Model. With the aim of computing failure probabilities, it is necessary to consider the probabilistic nature of strength properties and loads and the uncertainties in geometrical properties of the members. Without loss of generality of the procedure, in order to comply with the Hasofer-Lind hypothesis (Section 2.2), all the random variables are assumed as normally distributed. As the main purpose of the application of the procedure is the comparison between different design alternatives, the simplified assumption of normally distributed random variables has been regarded as appropriate for the problem at hand, in the understanding that adopting different probability distributions would not significantly affect the result.

For some quantities, a degradation model is adopted to reproduce the progressive decrease of mechanical characteristics due to damage. In this application, in order to account for corrosion mechanisms, the damage is considered to affect the steel rebars' yield strength (f_y), the area (A_s), and the steel girder yield strength (f_g). The degradation is represented by the following simplified relationships [50–52]:

$$A_s(t) = \left[1 - \delta_{A_s}(t)\right] A_{s,0}, \tag{4}$$

$$f_y(t) = \left[1 - \delta_{f_y}(t)\right] f_{y,0}, \tag{5}$$

$$f_g(t) = \left[1 - \delta_{f_g}(t)\right] f_{g,0}, \tag{6}$$

$$E_s(t) = \left[1 - \delta_{E_s}(t)\right] E_{s,0}, \tag{7}$$

where δ_{A_s}, δ_{f_s}, δ_{f_g}, and δ_{E_s} are dimensionless damage indexes which provide a measure of the damage level within the range $[0, 1]$ and $A_{s,0}$, $f_{y,0}$, $f_{g,0}$, and $E_{s,0}$ are the initial values of the deteriorating variables. The evolution with time of the damage indexes depends on the degradation process. Without loss of generality, different degradation models could be included in the procedure to describe the inherent complexity of the damage processes. Nonetheless, when comparing different design alternatives, the choice of a relatively simple model seems to be justifiable [52].

It is assumed that $\delta_{A_s} = \delta_{f_s} = \delta_{f_g} = \delta_{E_s} = \delta$, computed as

$$\delta = \begin{cases} \omega^{(1-\rho)} \tau^{\rho}, & \tau \le \omega, \\ \left(1 - (1-\omega)^{(1-\rho)}\right)(1-\tau)^{\rho}, & \omega < \tau < 1, \\ 1, & \tau \ge 1, \end{cases} \tag{8}$$

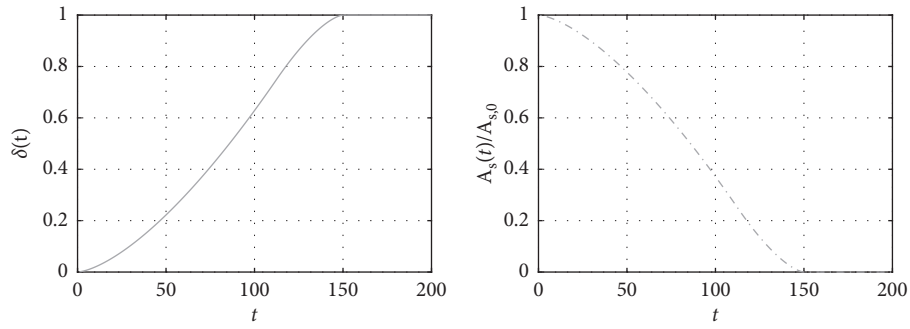

(a) (b)

Figure 8: Degradation model as a function of time (t) (a) and representation of the decrease of A_s with time expressed in years (b).

Table 1: Random variables used in the case study.

No.	Variable	Symbol	Mean value	CoV
1	Steel bar yield strength	$f_{y,0}$	570 MPa	0.052
2	Steel bar area	$A_{s,0}$	Nominal value	0.020
3	Steel girder yield strength	$f_{g,0}$	381.26 MPa	0.070
4	Deviation from concrete cover measure	Δc	1 cm	1.000
5	Concrete compression strength	f_c	36.55 MPa	0.180
6	Internal forces due to deck self-weight	V_1^D, M_1^D	Nominal values	0.010
7	Internal forces due to deck dead loads	V_2^D, M_2^D	Nominal values	0.025
8	Internal forces due to deck traffic loads	V_3^D, M_3^D	Nominal values	0.200
9	Internal forces due to girder self-weight	V_1^G, M_1^G, T_1^G	Nominal value	0.080
10	Internal forces due to girder dead loads	V_2^G, M_2^G, T_2^G	Nominal value	0.025
11	Internal forces and deflection due to global traffic loads	V_3^G, M_3^G, T_3^G, D_3^G	Nominal values	0.200
12	Internal forces and deflection due to wind	V_4^G, M_4^G, T_4^G, D_4^G	Nominal values	0.200
13	Internal forces and deflection due to thermal action	V_5^G, M_5^G, D_5^G	Nominal values	0.200

where $\omega = 0.75$, $\rho = 1.5$, $\tau = t/T_1$, and $T_1 = 150$ years, which is the time instant in which the failure threshold is reached. Figure 8(a) shows the coefficient δ as a function of time t, and Figure 8(b) shows the decrease of A_s with time (equation (5)).

Table 1 summarizes the parameters of the probabilistic distribution of random variables (mean values and standard deviations) that are used in this study. The parameters of variables 1 to 5 are taken from the probabilistic model code [53], while all the other parameters are taken from the literature [17, 29]. For time-dependent variables (from 1 to 3 in Table 1), the mean values of the distributions evolve according to equations (5)–(8). The standard deviations are considered as constant with time.

Since the loads vary around nominal (mean) values, the internal forces obtained through the structural analysis vary accordingly. The envelopes of the deformed shape, of the shear forces, and of the bending moments, obtained by varying the positions of the traffic loads along the deck and the girder, are computed from the FE models for each load case and for each one of the three construction phases. Figure 9 shows sample envelopes of the shear forces and bending moments in the deck corresponding to the envelope of LM2 and CL, for both design alternatives D1 and D2. The uncertainty in load characterization leads to variation of the envelope diagrams around the mean value.

3.5. Limit State Equations

3.5.1. Deck Limit States. The achievement of the ultimate bending moment and the ultimate shear force are the limit states taken into account for the reliability analysis of the deck.

The limit state function for bending is computed in any section of the deck as follows:

$$g_M^D(x) = A_s(x) f_y(x) 0.9 d(z) - \sum_i M_i^D(x), \tag{9}$$

where the coordinate x identifies the position along the transverse section, A_s is the area of rebars, f_y is the tensile yield stress, and M_i^D is the bending moment due to load case i on deck; d is given by

$$d(x) = H(x) - c - \Delta c, \tag{10}$$

where H is the section depth, c is the nominal value for the concrete cover, that is, 1 cm for lower reinforcements (due to the presence of predalles) and 4 cm for upper reinforcements, and Δc is a random variable expressing fluctuation of the concrete cover. All the items in equations (9) and (10) are random variables except for H and c that are assumed as deterministic.

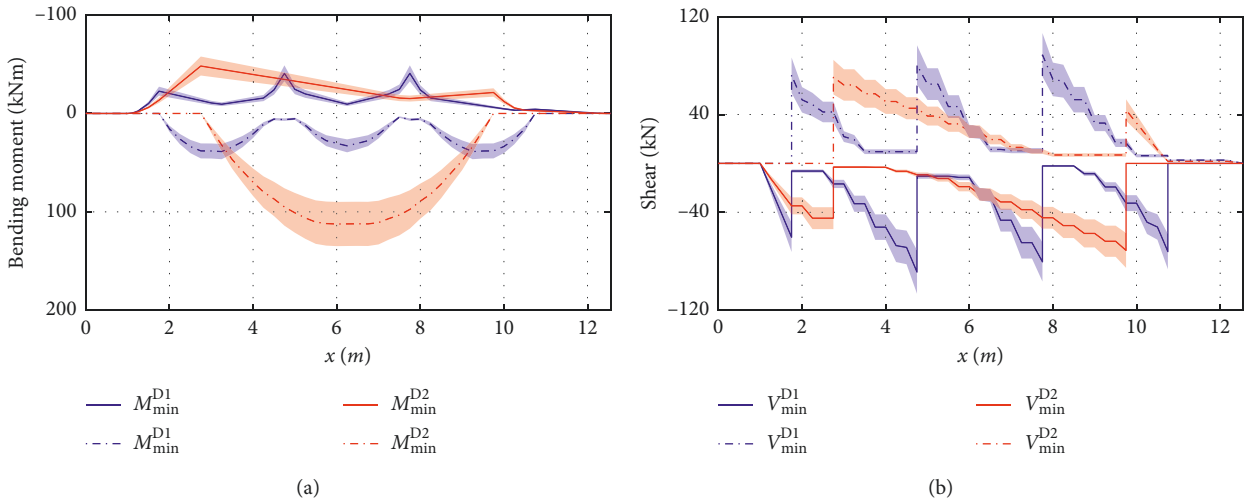

FIGURE 9: Envelopes of the bending moment and shear force in the deck for the two design alternatives (D1 and D2).

The limit state function for shear, is computed adopting the shear strength for concrete beams without stirrups, taken from the Eurocode 2 [46], given by

$$g_V^D(x) = \left\{0.18\left[1+\sqrt{\frac{200}{d(x)}}\right]\sqrt[3]{\frac{100A_s(x)f_c}{d(x)b}}\right\}bd(x) - \sum_i V_i^D(x), \tag{11}$$

where b is the width of the section, f_c is the concrete compression strength, and V_i^D is the shear force due to load case i acting on the deck. The random variables involved in equation (11) are $d(z)$, A_s, f_c, and V_i^D.

3.5.2. Girders Limit States. For girders analysis, three limit states have been considered: ultimate bending, ultimate shear (shear-torsion for model G1), and excessive deflection in long-term conditions (P3).

Bending strength corresponds to yield deformation of steel sections. The corresponding limit state equation can be written as follows:

$$g_M^G(y) = M_y^G(y) - \sum_i M_i^G(y), \tag{12}$$

where the coordinate y identifies the position on the longitudinal section, M_i^G is the bending moment due to load case i on girders, and M_y^G is the ultimate bending moment at yield deformation. The value of M_y^G depends on which part of the girder reaches the yield deformation first (concrete or steel). It in turn depends on the position of the neutral axis that does not depend on the applied stresses in the elastic field. Furthermore, if steel reaches the yield deformation before concrete, only the loads applied to steel have to be considered (i.e., steel-concrete self-weight). Thus, for M_y^G, the following equations can be used:

$$M_y^G(y) = \left[f_s - \frac{(\Sigma_{i=1}^2 M_i^G(y))y_s(y)}{J_s(y)}\right]\frac{J_{LT}(y)}{z_{LT}(y)} \quad \text{for } z_{LT}(y) < z_{cr}(y), \tag{13}$$

$$M_y^G(y) = f_c n\frac{J_{LT}(y)}{H - z_{LT}(y)} \quad \text{for } z_{LT}(y) > z_{cr}(y),$$

where f_s is the steel girders' yield stress, f_c is the concrete compression strength, n is the modular ratio, H is the total steel-concrete section height, z_{cr} is the neutral axis position for which top concrete and bottom steel reach the ultimate deformation and yield deformation, respectively, z_s and J_s are the neutral axis and moment of inertia of the steel section, and z_{LT} and J_{LT} are the neutral axis and moment of inertia for steel-concrete section homogenized with the long term modular ratio. Random variables involved in the girders' bending limit state are f_c, f_s, and M_i^G.

Shear limit state for girders can be expressed as follows:

$$g_V^G(y) = V_R^G(y) - \sum_i V_i^G(y), \tag{14}$$

where V_i^G is the shear due to load case i on girders, and V_R^G is the shear strength. The value of V_R^G is different in both alternatives because in ordinary double-T girders, only the web contributes to resistance, while in the box sections, the torque influence is not negligible. Thus, for V_R^G, the following expressions have been assumed:

$$V_R^G(y) = \frac{f_s A_v(y)}{\sqrt{3}}\left(1 - \frac{\sqrt{3}\sum_i T_i^G(y)}{2\Omega(y)f_s t(y)}\right) \quad \text{for G1,}$$

$$V_R^G(y) = \frac{A_v(y)f_s}{\sqrt{3}} \quad \text{for G2,} \tag{15}$$

where f_y^G is the steel yield stress, A_v is the shear area different for both alternatives, $T_i^G(x)$ is the torque at x-position due to load case i, Ω is the area inside the average line in thickness

of box sections, and t is the web thickness where shear stresses are maxima. Random variables involved in the girders' shear limit state are f_s, V_i^G, and T_i^G.

Deformability limit state concerns deflections due to variable load that in long terms leads to road surface damage. The limit state equation for deformability is the following:

$$g_D(y) = \frac{L}{350} - \sum_i D_i(y, A), \tag{16}$$

where D_i is the deflection due to the load case i (LM1, UDL, wind, and thermal load) at y-position on girders, depending on E_s (steel stiffness module) and J_{LT} (moment of inertia). Random variables involved in the girders' deformability limit state is D_i.

3.6. Cost Analysis. Total expected life-cycle cost is computed according to equations (1) and (2). A discount rate $r = 0.05$ is adopted.

3.6.1. Initial Costs. The initial cost C_I is taken from quantity surveys of the two design alternatives. Tables 2 and 3 summarize the initial costs of the two design alternatives for the deck and girders, respectively.

3.6.2. Repair Costs. For the computation of the repair costs, only direct costs are considered, as it is assumed that indirect repair costs are almost the same in the two design alternatives.

Expected values of direct repair costs $E[C_R(t)]$ are defined as in equation (2). The repair cost of a structural element, for damage related to the j-th limit state, can be computed as a fraction α of the initial cost C_I, as follows:

$$c_{R,j} = \alpha C_I. \tag{17}$$

The cost $c_{R,j}$ is considered as a unit cost referred to a reference length L_j across the considered section. Without loss of generality, it is assumed $L_j = 2$ m for the limit states related to the deck and $L_j = 12$ m for the limit states related to the girders. The coefficient α is taken to be equal to 0.2 for the deformability limit state and equal to 1.1 for all other limit states, to account also for disposal costs [54].

4. Results of the Reliability Analysis

The reliability index is computed according to the FORM method, as illustrated in Section 2.2. At first, the degradation of the materials is neglected and the failure probability is considered to be independent of time.

With reference to the deck model, β is computed for each output node along the transverse section and for the two design alternatives (D1 and D2). Figure 10 compares the envelopes of the reliability indexes at any reference section for the bending moment limit state (Figure 10(a)) and shear limit state (Figure 10(b)) for D1 and D2. It is possible to observe that the design alternative D2 has smaller reliability index for both bending and shear limit states. The shear limit state is the one providing a smaller reliability index. The β diagrams do not have the same trend as the internal forces (cf. Figure 9) because β locally depends on the reinforcement. This result highlights that the main advantage of the proposed procedure is its ability to provide local reliability indexes and therefore to locally check the achievement of a limit state. Indeed, as it can be seen from Figure 9, it may happen that the reliability index exhibits local or global minima in sections where there is a change in geometry or reinforcements.

Table 2: Initial costs of the two design alternatives for the deck.

Cost item	Cost in alternative 1 (€)	Cost in alternative 2 (€)
Construction	695.509	1.011.634
Safety burdens	52.017	102.348
Terrain purchase	12.378	12.378
Testing	20.865	30.349
Design	48.685	70.814
Total initial cost C_I	829.454	1.227.523

Table 3: Initial costs of the two design alternatives for the girders.

Cost item	Cost in alternative 1 (€)	Cost in alternative 2 (€)
Construction	4.673.660	3.331.431
Safety burdens	349.548	337.046
Terrain purchase	83.182	83.182
Testing	140.209	99.942
Design	327.156	233.200
Total initial cost	5.573.755	4.084.801

Regarding the girder model, β is computed for each output node and for the two design alternatives (G1 and G2). Figure 11 shows the envelopes of the minimum reliability index at any reference section for the bending moment limit state (Figure 11(a)), shear limit state (Figure 11(b)), and deformability limit state (Figure 11(c)). Also, for the girder analysis it can be inferred that the design alternative G2 has a smaller reliability index. The different positions of local maxima in the graphs are due to the different lengths of the free spans in the two design alternatives (Figure 3). The bending limit state is the one leading to a smaller reliability index.

Table 4 summarizes the minimum β indexes with the corresponding failure probabilities P_f for the analyzed limit states and the two design alternatives. It also reported the position from the left bound of the structure x (for the deck) and y (for the girder) at which the minimum β (maximum failure probability) occurs.

In order to highlight the effect of considering the materials' degradation, the reliability analysis has been repeated by taking into account the time-dependent random variables, as in equations (5)–(8). Figure 12 shows the β indexes for deck bending and shear limit states at the initial construction time ($t = 0$) and after 30 and 60 years. It can be observed that the β index significantly decreases with time. While in alternative D2 just after construction ($t = 0$), the smallest reliability index is

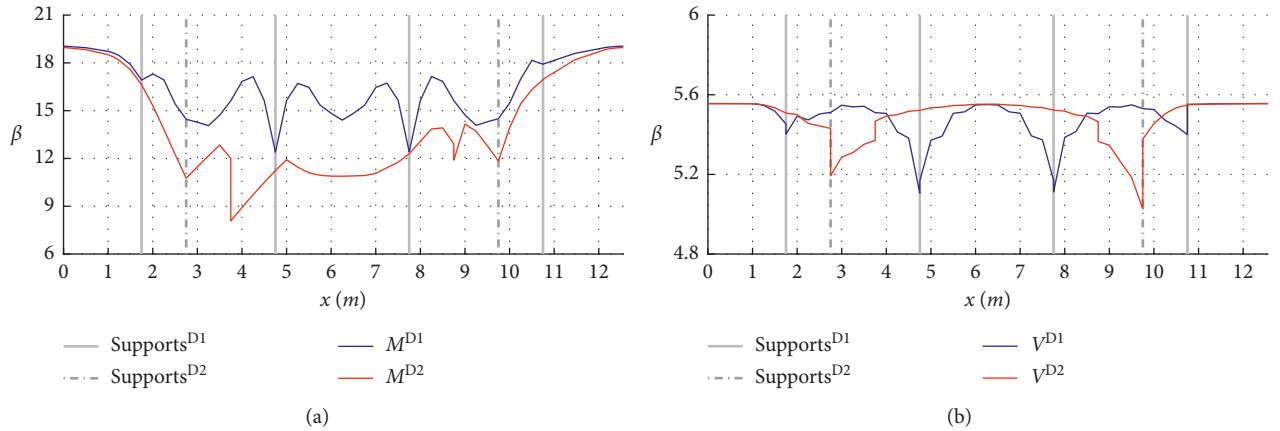

FIGURE 10: Reliability index β for the deck in the two design alternatives: related to the bending limit state (a) and to the shear limit state (b).

for shear, after 60 years the bending becomes the limit state providing the smallest level of safety. β changes with the increase in time. Similar results can be inferred from Figure 13 showing the evolution with time of the β indexes for bending, shear, and deformability limit states at the initial construction time ($t = 0$) and after 30 and 60 years. The decrease with time of the reliability indexes related to bending and shear limit states is greater than that related to deformability. Table 5 summarizes the minimum β indexes for the two design alternatives and for the different analyzed lifetimes. After 60 years, the β indexes of some limit states drop below values considered unacceptable by technical standards (corresponding to failure probabilities higher than 10^{-5}). The result is strictly dependent on the damage model chosen to represent material's degradation, highlighting the need of correctly predicting the evolution of damage in the specific site conditions. The results in terms of local reliability index emphasize the utility of the proposed procedure in identifying the most critical locations and limit states, with the main aim to decide the priority of intervention that is strongly dependent on the structural details of the deck and on the material's degradation model.

5. Results of the Cost Analysis

In this Section, the total expected life-cycle cost is computed trough the proposed procedure, based on the results of the reliability analysis. Maintenance costs are neglected, as they do not vary significantly in the two design alternatives. Therefore, without loss of generality, equation (1) is simplified as follows:

$$E[C(t_l)] = C_I + \sum_{t=1}^{t_l} \frac{E[C_R(t)]}{(1+r)^t}. \quad (18)$$

The time-dependent probabilities of failure $P_{j,k}^{f}(t)$ are used to compute the expected repair costs, according to equation (2). Figure 14 shows the expected repair costs over its lifetime for the deck (a) and the girder (b), for the two design alternatives. It can be observed that the repair costs are higher for design alternative 2 for lifetimes higher than about 60 years. This is due to the higher failure probabilities that pertain to D2 and G2, with respect to D1 and G1, as highlighted in Figures 12 and 13. Figure 15 shows the expected total costs as a function of lifetime in the two design alternatives. In particular, Figure 15(a) compares the initial and total expected repair costs for the two alternatives, and Figures 15(b) and 15(c) show the total cost increase with respect to the initial cost for the two design alternatives. It is possible to observe that the increase in cost with respect to initial costs is much higher for design alternative 2. However, for lifetimes lower than about 95 years, alternative 2 is the most economic, as the total expected cost is smaller than that in alternative 1. Conversely, for lifetimes greater than about 95 years, the total expected cost is greater for alternative 2. Indeed, if the costs are evaluated in a life-cycle perspective, a design solution initially considered the most economic can reveal to be the most expensive. The procedure gives quantitative information to decide which is the most effective solution from the life-cycle cost point of view, highlighting at the same time which are the deck and girder cross sections, where maintenance interventions are needed with priority.

6. Parametric Analysis

In order to study the influence of the degradation model described in equations (5)–(8), a parametric analysis is carried out by varying the time corresponding to the failure threshold T1 from 100 to 250 years, with $\omega = 0.75$ and $\rho = 1.5$. The following degradation models (DM) are analyzed and compared: DM1 with $T_1 = 100$; DM2 with $T_1 = 150$; DM3 with $T_1 = 200$; and DM4 with $T_1 = 250$.

Moreover, to account for the fact that corrosion can have a different effect on the steel area reduction A_s with respect to other mechanical parameters like f_y, f_g, and E_s, an additional model (DM5) is introduced in the analysis. In this last case, according to equation (8), the damage index δ_{A_s} is evaluated by considering $T_1 = 150$, while δ_{f_s}, δ_{f_g}, and δ_{E_s} are evaluated with $T_1 = 250$.

Numerical results reported in Table 6 summarize the minimum values of β for the two design alternatives and for $t = 30$ years obtained for different degradation models. It can be observed that the degradation model has a significant

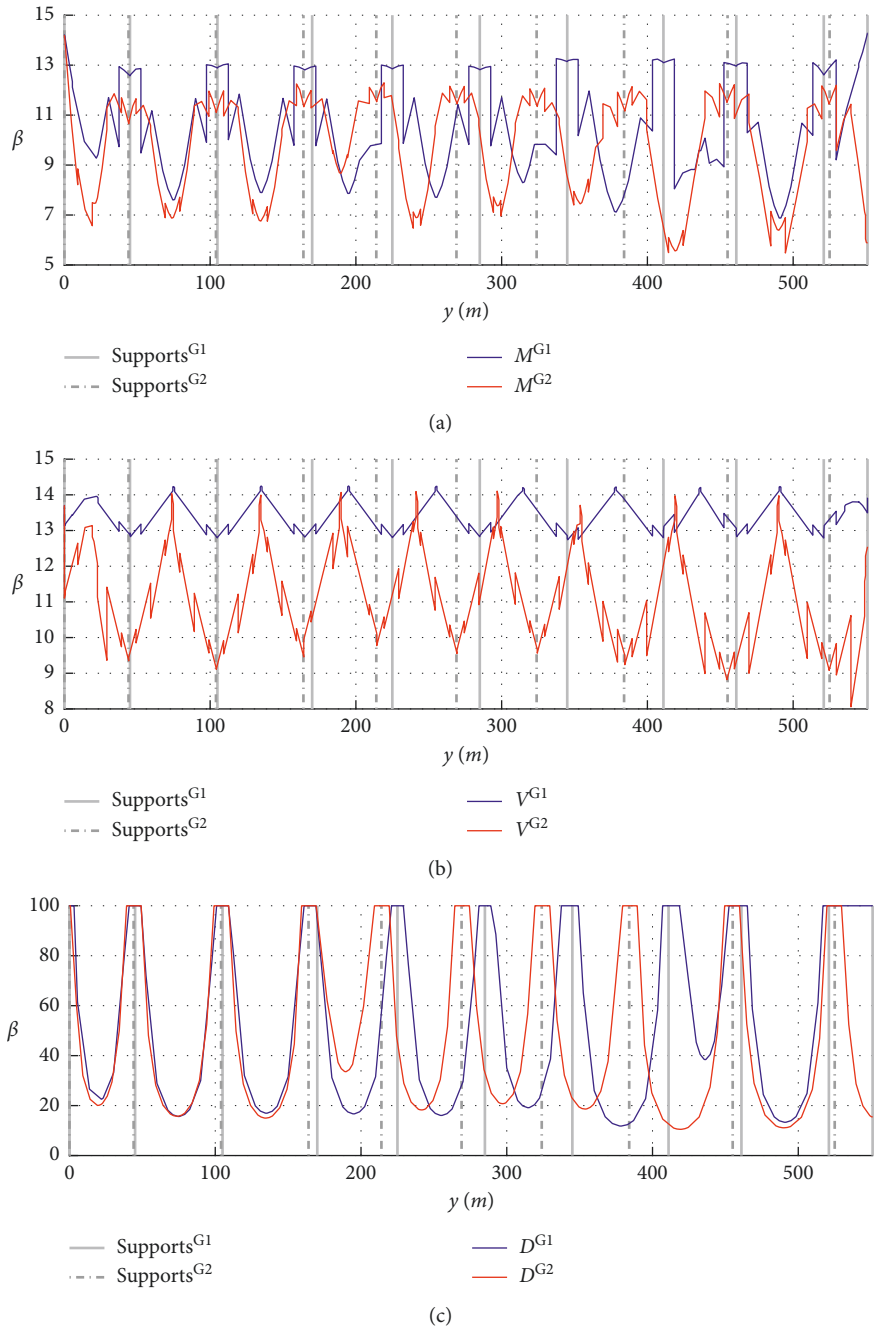

Figure 11: Reliability index β for girders in the two design alternatives: related to the bending limit state (a); to the shear limit state (b); and to the deformability limit state (c).

Table 4: Results of the reliability analysis for the two design alternatives.

Limit state	D1			D2		
	β	P_f	x	β	P_f	x
Bending deck	12.39	$1.37e-35$	4.75	8.08	$3.20e-16$	3.75
Shear deck	5.10	$1.64e-07$	4.75	5.02	$2.49e-07$	9.78
Limit state	G1			G2		
	β	P_f	y	β	P_f	y
Bending girder	6.88	$3.03e-12$	491.00	5.48	$2.13e-08$	494.66
Shear girder	12.74	$1.77e-37$	345.30	8.06	$3.88e-16$	539.64
Deformability girder	11.81	$1.69e-32$	378.60	10.50	$4.40e-26$	418.94

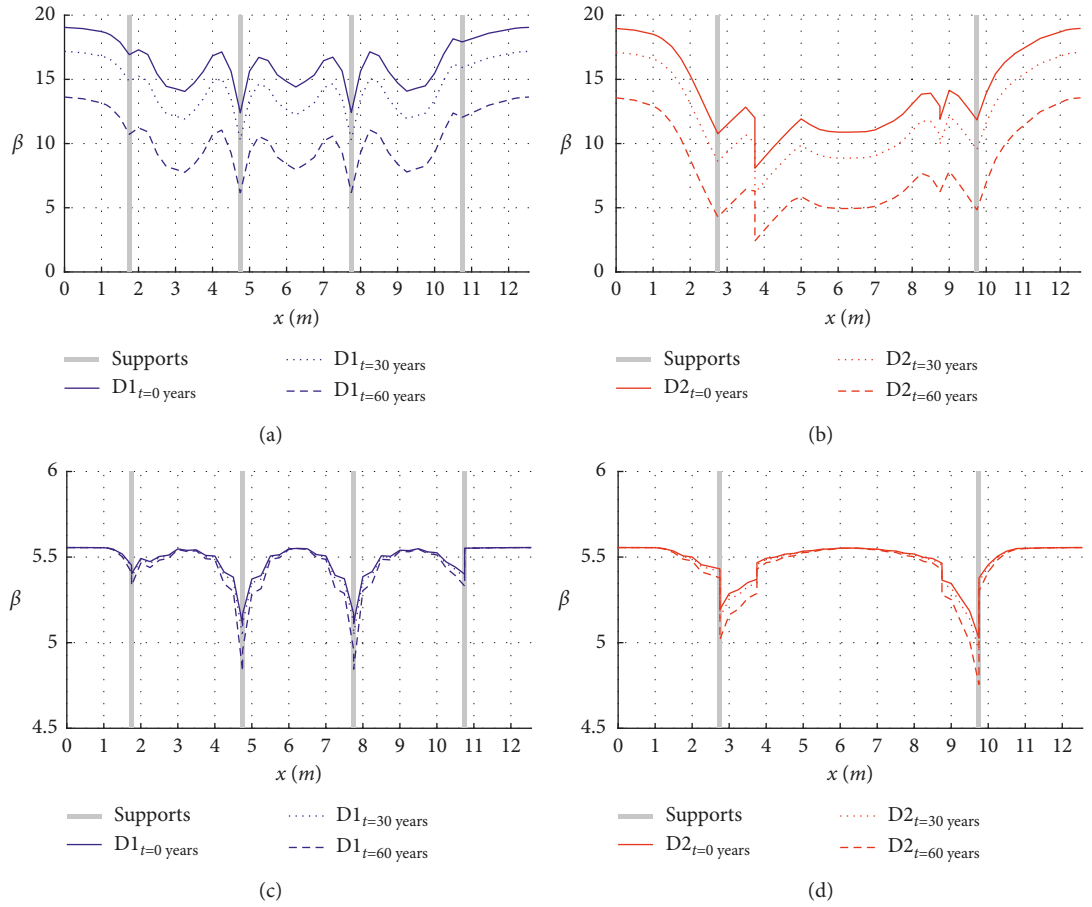

Figure 12: Reliability index for the deck for different lifetimes.

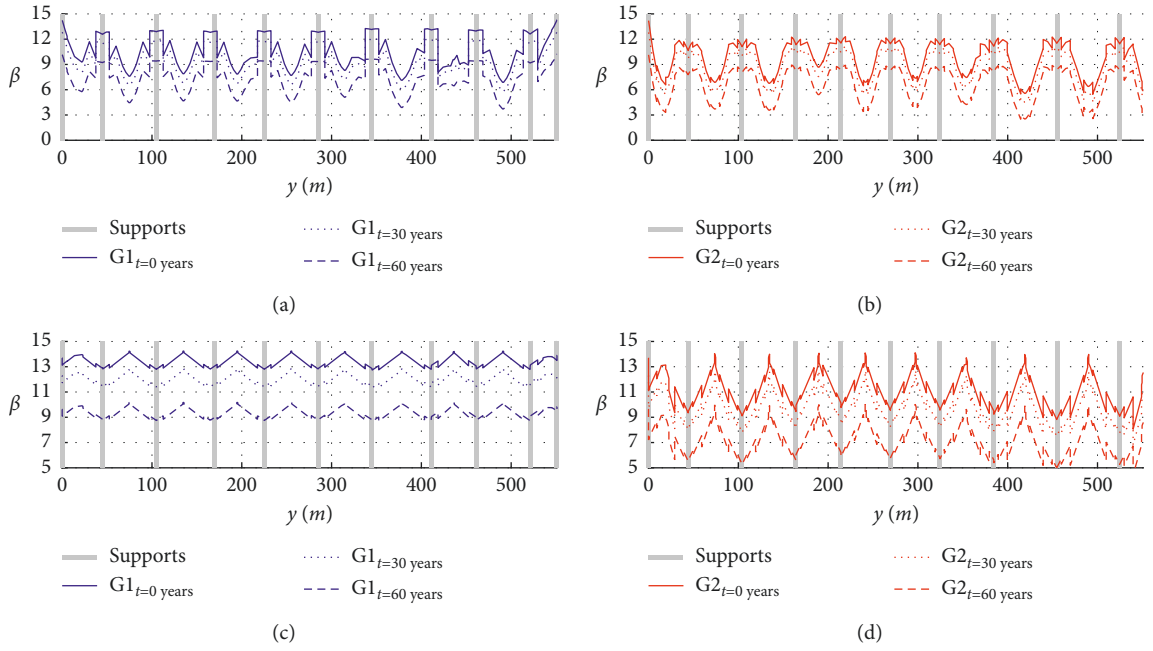

Figure 13: Continued.

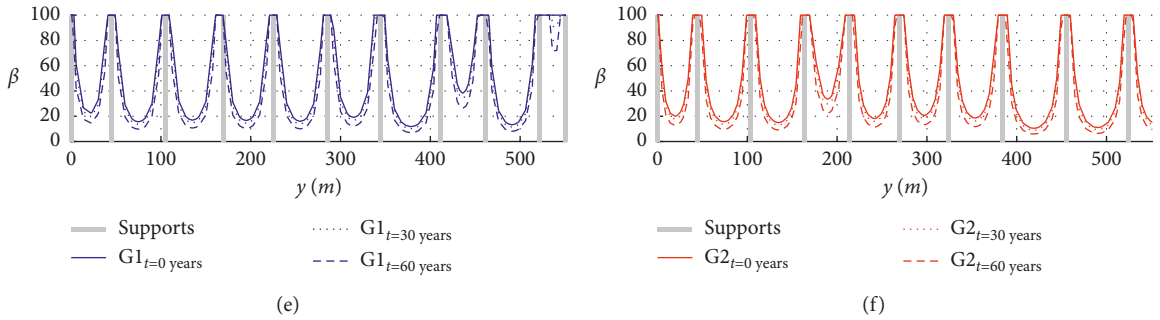

Figure 13: Reliability index for the girder for different lifetimes.

Table 5: Minimum β indexes for the two design alternatives and for different lifetimes.

Limit state	$t = 0$ year		$t = 30$ years		$t = 60$ years	
	D1	D2	D1	D2	D1	D2
Bending deck	12.39	8.08	10.27	6.16	6.14	2.41
Shear deck	5.10	5.02	5.04	4.95	4.83	4.75
Limit state	G1	G2	G1	G2	G1	G2
Bending girder	6.87	5.48	5.80	4.46	3.72	2.30
Shear girder	12.74	8.06	11.34	6.81	8.68	4.43
Deformability girder	11.81	10.50	10.16	8.94	7.02	5.96

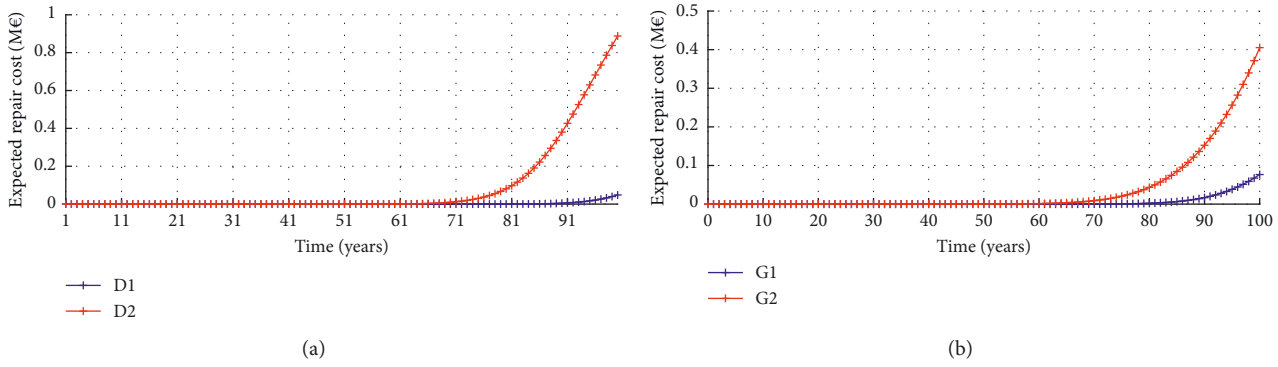

Figure 14: Expected repair costs over a lifetime for the deck (a) and the girder (b), for the two design alternatives.

influence on the reliability index. In particular, as the failure time threshold T_1 increases, the reliability index consequently increases. The degradation model has greater influence on reliability related to bending than on reliability related to shear or deformability. The effect of different degradation models on life-cycle costs is also investigated. Figure 16 depicts the expected repair costs for design alternatives 1 and 2, considering the five deterioration models and different lifetimes (t = 60, 80, and 100 years). It is possible to observe the significant influence of the choice of the degradation model on the estimated repair cost, which reflects the expected influence of the degradation rate on the repair costs, also highlighting that repair costs are strongly influenced by the aggressiveness of the environment.

7. Conclusions

The present paper has proposed a procedure for the life-cycle cost analysis of road girder bridges. The life-cycle cost is related to the failure probability which is locally and automatically computed along the entire bridge deck for several limit states. The procedure accounts in a simplified way for material degradation by introducing the dependency on time of several damage-dependent parameters. Load and strength parameters are considered uncertain with a normal probability distribution. Design traffic actions on the bridge suggested by international technical standards are also adopted considering the interaction between deck and girder loads. Different construction phases of composite steel-

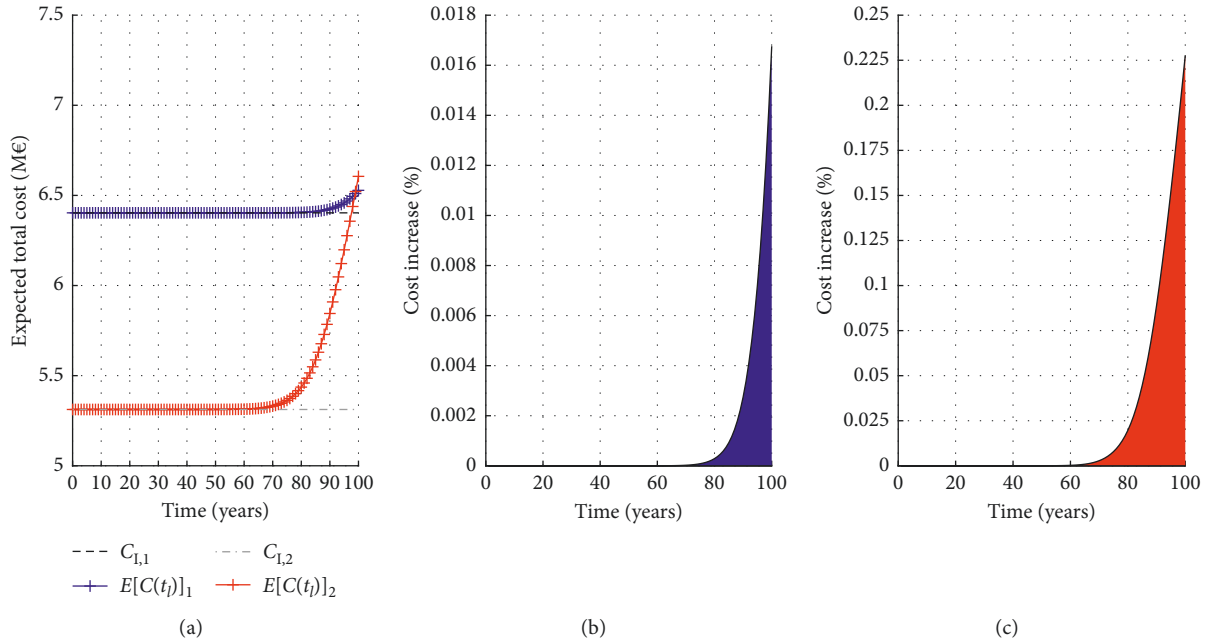

Figure 15: (a) Expected total costs of the two design alternatives compared with the corresponding initial costs; (b) total cost increase with respect to initial cost in design alternative 1 and (c) and total cost increase with respect to initial cost in design alternative 2.

Table 6: Minimum β indexes for the two design alternatives and for $t = 30$ years for different degradation models.

Limit state	DM1		DM2		DM3		DM4		DM5	
	D1	D2	D1	D2	D1	D2	D1	D2	D1	D2
Bending deck	8.69	4.72	10.27	6.16	11.20	6.84	11.41	7.19	10.99	6.73
Shear deck	4.97	4.89	5.04	4.95	5.07	4.98	5.08	4.99	5.04	4.95
Limit state	G1	G2	G1	G2	G1	G2	G1	G2	G1	G2
Bending girder	5.00	3.62	5.80	4.46	6.27	4.83	6.38	5.02	6.34	5.01
Shear girder	10.32	5.89	11.34	6.81	11.95	7.25	12.09	7.48	12.09	7.48
Deformability girder	8.95	7.79	10.16	8.94	10.88	9.48	11.04	9.77	11.04	9.77

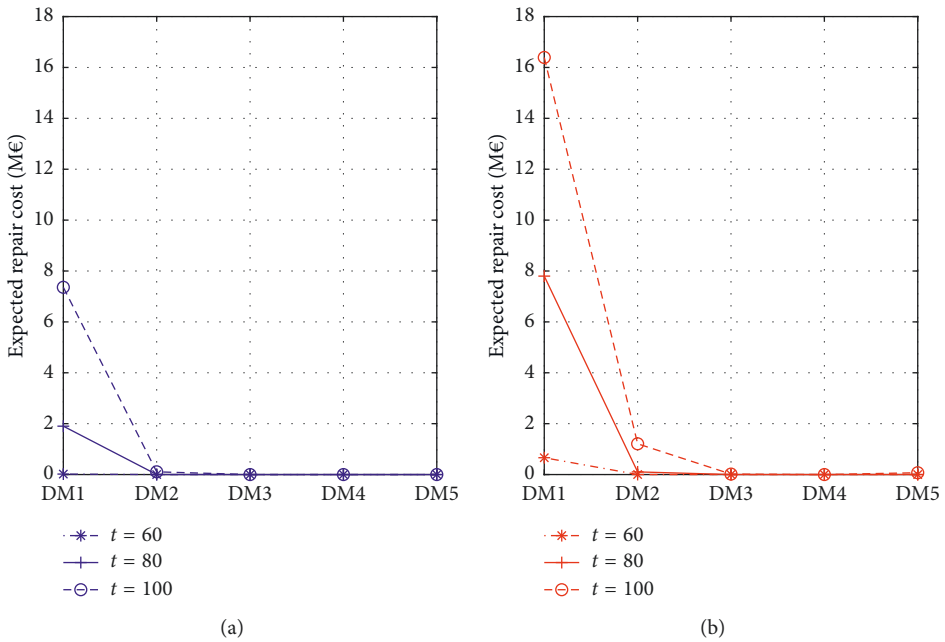

Figure 16: Expected repair costs for different deterioration models and for $t = 60, 80, 100$: (a) design alternative 1 and (b) design alternative 2.

reinforced concrete beams are analyzed. Reliability analysis is carried out for all the considered limit states and in correspondence of each location along the deck and the girder, to provide local values of the reliability index and failure probability. The procedure is applied to a case study of a road bridge for which, in the design phase, two different design alternatives were proposed. Results show that the reliability index is strongly dependent on the considered limit state and on the structural details of the deck, thus emphasizing the importance of the local reliability assessment, in order to estimate the priority and timing of interventions. The computation of the expected life-cycle cost allows a quantitative comparison between the two different design alternatives in a life-cycle perspective. The choice of the most economic solution strongly depends of the lifetime expected for the structure and on the degradation model adopted to account for material's deterioration.

Data Availability

The numerical data used to support the findings of this study are available from the corresponding author upon request.

Conflicts of Interest

The authors declare that they have no conflicts of interest.

References

[1] C. Liu, Y. Gong, S. Laflamme, B. Phares, and S. Sarkar, "Bridge damage detection using spatiotemporal patterns extracted from dense sensor network," *Measurement Science and Technology*, vol. 28, no. 1, article 014011, 2016.

[2] Y. K. Wen and Y. J. Kang, "Minimum building life-cycle cost design criteria. I: Methodology," *Journal of Structural Engineering*, vol. 127, no. 3, pp. 330–337, 2001.

[3] D. M. Frangopol, Y. Dong, and S. Sabatino, "Bridge life-cycle performance and cost: analysis, prediction, optimisation and decision-making," *Structure and Infrastructure Engineering*, vol. 13, no. 10, pp. 1239–1257, 2017.

[4] D. M. Frangopol, "Life-cycle performance, management, and optimisation of structural systems under uncertainty: accomplishments and challenges1," *Structure and Infrastructure Engineering*, vol. 7, no. 6, pp. 389–413, 2011.

[5] N. Okasha and D. M. Frangopol, "Computational platform for the integrated life-cycle management of highway bridges," *Engineering Structures*, vol. 33, no. 7, pp. 2145–2153, 2011.

[6] L. Ierimonti, L. Caracoglia, I. Venanzi, and A. L. Materazzi, "Investigation on life-cycle damage cost of wind-excited tall buildings considering directionality effects," *Journal of Wind Engineering and Industrial Aerodynamics*, vol. 171, pp. 207–218, 2017.

[7] L. Gao, Y. Li, and J. Hu, "Life-cycle cost framework analysis for a bridge," *WIT Transactions on the Built Environment*, vol. 140, pp. 85–88, 2013.

[8] D. M. Frangopol and M. Soliman, "Life-cycle of structural systems: recent achievements and future directions," *Structure and Infrastructure Engineering*, vol. 12, no. 1, pp. 1–20, 2015.

[9] S.-H. Kim, M.-S. Choi, K.-I. Cho, and S.-J. Park, "Determining the optimal structural target reliability of a structure with a minimal life-cycle cost perspective," *Advances in Structural Engineering*, vol. 16, no. 12, pp. 2075–2091, 2016.

[10] M. Stewart, "Reliability-based assessment of ageing bridges using risk ranking and life cycle cost decision analyses," *Reliability Engineering and System Safety*, vol. 74, no. 3, pp. 263–273, 2001.

[11] C. D. Eamon, E. A. Jensen, N. F. Grace, and X. Shi, "Life-cycle cost analysis of alternative reinforcement materials for bridge superstructures considering cost and maintenance uncertainties," *Journal of Materials in Civil Engineering*, vol. 24, no. 4, pp. 373–380, 2012.

[12] K. Ozbay, D. Jawad, N. Parker, and S. Hussain, "Life-cycle cost analysis: State of the practice versus state of the art," *Transportation Research Record*, vol. 1864, no. 1, pp. 62–70, 2004.

[13] M. Akiyama, D. M. Frangopol, and K. Takenaka, "Reliability-based durability design and service life assessment of reinforced concrete deck slab of jetty structures," *Structure and Infrastructure Engineering*, vol. 13, no. 4, pp. 468–477, 2016.

[14] L. Ierimonti, I. Venanzi, and L. Caracoglia, "Life-cycle damage-based cost analysis of tall buildings equipped with tuned mass dampers," *Journal of Wind Engineering and Industrial Aerodynamics*, vol. 176, pp. 54–64, 2018.

[15] Y. K. Wen, "Minimum lifecycle cost design under multiple hazards," *Reliability Engineering and System Safety*, vol. 73, no. 3, pp. 223–231, 2001.

[16] I. Venanzi, O. Lavan, L. Ierimonti, and S. Fabrizi, "Multi-hazard loss analysis of tall buildings under wind and seismic laods," *Structure and Infrastructure Engineering*, vol. 14, no. 10, pp. 1295–1311.

[17] K.-M. Lee, H.-N. Cho, and Y.-M. Choi, "Life-cycle cost-effective optimum design of steel bridges," *Journal of constructional steel research*, vol. 60, no. 11, pp. 1585–1613, 2004.

[18] M. Jiang, R. Corotis, and H. Ellis, "Optimal life-cycle costing with partial observability," *Journal of Infrastructure Systems*, vol. 6, no. 2, pp. 56–66, 2001.

[19] L. Saad, A. Aissani, A. Chateauneuf, and W. Raphael, "Reliability-based optimization of direct and indirect LCC of RC bridge elements under coupled fatigue-corrosion deterioration processes," *Engineering Failure Analysis*, vol. 59, pp. 570–587, 2016.

[20] J. J. Veganzones Muñoz, L. Pettersson, H. Sundquist, and R. Karoumi, "Life-cycle cost analysis as a tool in the developing process for new bridge edge beam solutions," *Structure and Infrastructure Engineering*, vol. 12, no. 9, pp. 1185–1201, 2016.

[21] N. Ta, A. Orcesi, and C. Cremona, "A comparative life-cycle cost analysis of steel-concrete composite bridges," in *Life-Cycle and Sustainability of Civil Infrastructure Systems: Proceedings of the 3rd International Symposium on Life-Cycle Civil Engineering*, pp. 696–702, Vienna, Austria, October 2012.

[22] S.-H. Han, W.-S. Lee, and M.-S. Bang, "Probabilistic optimal safety with minimum life-cycle cost based on stochastic finite element analysis of steel cable-stayed bridges," *International Journal of Steel Structures*, vol. 11, no. 3, pp. 335–349, 2011.

[23] Y. S. Shin, J. H. Park, and D.-H. Ha, "Optimal design of a steel box girder bridge considering life cycle cost," *KSCE Journal of Civil Engineering*, vol. 13, no. 6, pp. 433–440, 2009.

[24] M. E. Fagen and B. M. Phares, "Life-cycle cost analysis of a low-volume road bridge alternative," *Transportation Research Record: Journal of the Transportation Research Board*, vol. 1696, no. 1, pp. 8–13, 2018.

[25] M. S. Bang, "Optimal design of suspension bridge based on minimization of life cycle cost," *Advanced Materials Research*, vol. 919-921, pp. 577–582, 2014.

[26] T. Garca-Segura, V. Yepes, and D. Frangopol, "Multi-objective design of post-tensioned concrete road bridges using artificial neural networks," *Structural and Multidisciplinary Optimization*, vol. 56, no. 1, pp. 139–150, 2017.

[27] J. E. Padgett, K. Dennemann, and J. Ghosh, "Risk-based seismic life-cycle cost-benefit (LCC-B) analysis for bridge retrofit assessment," *Structural Safety*, vol. 32, no. 3, pp. 165–173, 2010.

[28] M. Liu and D. M. Frangopol, "Optimizing bridge network maintenance management under uncertainty with conflicting criteria: life-cycle maintenance, failure, and user costs," *Journal of Structural Engineering*, vol. 132, no. 11, pp. 1835–1845, 2006.

[29] S. Sabatino, D. M. Frangopol, and Y. Dong, "Sustainability-informed maintenance optimization of highway bridges considering multi-attribute utility and risk attitude," *Engineering Structures*, vol. 102, pp. 310–321, 2015.

[30] J. O. Almeida, P. F. Teixeira, and R. M. Delgado, "Life cycle cost optimisation in highway concrete bridges management," *Structure and Infrastructure Engineering*, vol. 11, no. 10, pp. 1263–1276, 2013.

[31] B. Le and J. Andrews, "Petri net modelling of bridge asset management using maintenance-related state conditions," *Structure and Infrastructure Engineering*, vol. 12, no. 6, pp. 730–751, 2015.

[32] Á. Cunha, E. Caetano, F. Magalhães, and M. Carlos, "Dynamic identification and continuous dynamic monitoring of bridges: different applications along bridges life-cycle," *Structure and Infrastructure Engineering*, vol. 14, no. 4, pp. 445–467, 2017.

[33] G. Moutinho, D. Frangopol, and M. Soliman, "Optimization of life-cycle maintenance of deteriorating bridges with respect to expected annual system failure rate and expected cumulative cost," *Journal of Structural Engineering (United States)*, vol. 140, no. 4, article 04013043, 2017.

[34] A. Hatami and G. Morcous, "Deterioration models for life-cycle cost analysis of bridge decks in Nebraska," *Transportation Research Record*, vol. 2313, no. 1, pp. 3–11, 2012.

[35] P. Liu, "Life cycle cost analysis of anticorrosive coating of steel bridge," *Advanced Materials Research*, vol. 496, pp. 121–125, 2012.

[36] N. M. Okasha, D. M. Frangopol, F. B. Fletcher, and A. D. Wilson, "Life-cycle cost analyses of a new steel for bridges," *Journal of Bridge Engineering*, vol. 17, no. 1, pp. 168–172, 2012.

[37] R. Bhaskaran, N. Palaniswamy, and N. Rengaswamy, "Life-cycle cost analysis of a concrete road bridge across open sea," *Materials Performance*, vol. 45, pp. 51–55, 2006.

[38] D. M. Frangopol, K.-Y. Lin, and A. C. Estes, "Life-cycle cost design of deteriorating structures," *Journal of Structural Engineering*, vol. 123, no. 10, pp. 1390–1401, 1997.

[39] A. N. Kallias, B. Imam, and M. K. Chryssanthopoulos, "Performance profiles of metallic bridges subject to coating degradation and atmospheric corrosion," *Structure and Infrastructure Engineering*, vol. 13, no. 4, pp. 440–453, 2016.

[40] M. Safi, H. Sundquist, and R. Karoumi, "Cost-efficient procurement of bridge infrastructures by incorporating life-cycle cost analysis with bridge management systems," *Journal of Bridge Engineering*, vol. 20, no. 6, article 04014083, 2015.

[41] M. Safi, H. Sundquist, R. Karoumi, and G. Racutanu, "Integration of life-cycle cost analysis with bridge management systems," *Transportation Research Record: Journal of the Transportation Research Board*, vol. 2292, no. 1, pp. 25–133, 2018.

[42] H. S. Shim and S. H. Lee, "Developing a probable cost analysis model for comparing bridge deck rehabilitation methods," *KSCE Journal of Civil Engineering*, vol. 20, no. 1, pp. 68–76, 2015.

[43] P. Thoft-Christensen, "Life-cycle cost-benefit (LCCB) analysis of bridges from a user and social point of view," *Structure and Infrastructure Engineering*, vol. 5, no. 1, pp. 49–57, 2009.

[44] K. Lee, H. Cho, and C. Cha, "Life-cycle cost-effective optimum design of steel bridges considering environmental stressors," *Engineering Structures*, vol. 28, no. 9, article 12521265, 2006.

[45] The MathWorks Inc., *MATLAB R2009b: Release Note User's GUIDE*, The MathWorks, Inc., Natick, MA, USA, 2009.

[46] European Committee for Standardization, *1992-1-1:2005-Eurocode 2-Design of Concrete Structures-Part 1-1: General Rules and Rules for Buildings*, European Committee for Standardization, 36 rue de Stassart, B 1050 Brussels, 2005.

[47] European Committee for Standardization, *1994-1-1:2004-Eurocode 4: Design of Composite Steel and Concrete Structures-Part 1-1: General Rules and Rules for Buildings*, European Committee for Standardization, 36 rue de Stassart, B 1050 Brussels, 2004.

[48] European Committee for Standardization, *1991-1:2003-Eurocode 1: Actions on Structures-Part 1-1: General actions-Densities, Self-Weight, Imposed Loads for Buildings*, European Committee for Standardization, 36 rue de Stassart, B 1050 Brussels, 2003.

[49] European Committee for Standardization, *1991-2:2003-Eurocode 1: Actions on Structures-Part 1-2: Traffic Loads On Bridges*, European Committee for Standardization.

[50] F. Biondini and G. Zani, "Life-cycle multi-objective optimization of deteriorating structures," in *Life Cycle Civil Engineering*, pp. 285–291, Taylor F. Group, London, UK, 2008.

[51] F. Biondini and D. Frangopol, "Life-cycle multi-objective optimization of deteriorating structures," in *Life Cycle Civil Engineering*, pp. 285–291, Taylor F. Group, London, UK, 2008.

[52] F. Biondini and A. Marchiondelli, "Evolutionary design of structural systems with time-variant performance," *Structure and Infrastructure Engineering*, vol. 4, no. 2, pp. 163–176, 2008.

[53] Joint Committee on Structural Safety, *Probabilistic Model Code, Chap. Part 3: Material Properties*, Joint Committee on Structural Safety, 2000.

[54] S. Noponen and A. Jutila, "LCC case studies for bridges in different design phases," in *Life Cycle Civil Engineering*, pp. 851–856, Taylor and Francis Group, London, UK, 2008.